Ninth International Conference on CFD in the Minerals and Process Industries
CSIRO, Melbourne, Australia
10-12 December 2012

USING CFD TO SIMULATE HEAT TRANSFER IN PARTICLE CURTAINS

Sepideh AFSHAR[1*] and Madoc SHEEHAN[1]

[1]Department of Chemical Engineering, James Cook University, Townsville, Queensland 4811, AUSTRALIA
*Corresponding author, E-mail address: sepideh.afshar@my.jcu.edu.au

ABSTRACT

Particle curtains are very common in industrial drying, particularly in the minerals industry. Flighted rotary dryers are typical industrial unit operations in which particle curtains interact with hot air and undergo both convection and evaporation. Furthermore, there are many examples within industrial processing where streams of hot particles could be used to extract or reclaim energy. However, our understanding of heat transfer in falling curtains is limited by the complexity of curtain behaviour in comparison to the behaviour of single particles. Falling curtains exhibit convergent and divergent behaviour depending on inlet conditions and particle properties. The initial thickness of a curtain at discharge and the curtain flow rate have significant effects on the shapes of falling curtains and lead to varying rates of convective heat transfer. In this work 3-D Eulerian-Eulerian CFD is used to simulate convective heat transfer in free falling particle curtains. Total heat loss for curtaining particles falling a fixed distance is compared to heat loss for isolated single particles. Hot spherical silica particles with density of 2634 kg/m^3 at 400K (200 µm, 400 µm and 600µm) flow at approximately 0.041 kg/s to 0.2 kg/s through a narrow slot in a rectangular box (0.45m×0.9m×0.225 m) filled with ambient air. The slot sizes through which the particles enter the rectangular box were 10mm, 30mm, 60mm and 80mm. Mesh dependency was performed by comparing the average properties of the falling curtain such as total heat loss per unit mass, as a function of mesh size. Mesh dependency was found to be independent of convergence and divergence of particle curtains and a 4mm mesh size was selected. The results for total heat loss at different slot sizes in the particle curtain simulations were compared to commonly used single particle heat transfer models. The results showed that modifying the inlet slot width at 0.041kg/s for 400µm particles can lead to 13% increases in rates of convective heat transfer per unit mass.

NOMENCLATURE

A	area,[m^2]
C_D	drag coefficient,[-]
C_p	specific heat capacity ,[J.kg^{-1}.K^{-1}]
d	diameter,[m]
e_s	restitution coefficient of particles,[-]
F_D	drag force (N)
F_G	gravity force (N)
g	acceleration due to gravity,9.81[m.s^{-2}]
g_0	radial distribution function,[-]
h	convective heat transfer coefficient,[J.m^{-2}.K^{-1}]
$\overline{\overline{I}}$	unit stress tensor,[-]
k	turbulence kinematic energy per unit mass,[m^2.s^{-2}]
m	mass,[kg]
m^0	mass flow rate, [kg.s^{-1}]
Nu	Nusselt number,[-]
P	pressure,[Pa]
Pr	Prandtl number,[-]
$G_{kb,g}$	turbulence production due to buoyant forces,[kg.m^{-1}.s^{-3}]
$G_{k,g}$	turbulence production due to viscous and buoyant forces,[kg.m^{-1}.s^{-3}]
Re	Reynolds number,[-]
T	temperature,[K]
T	transpose,[-]
$T_{gs}^{(k)}, T_{gs}^{(\varepsilon)}$	influence of dispersed phase on continuous phase,[-]
t	time,[s^{-1}]
v	velocity,[m.s^{-1}]
v'	fluctuating velocity,[m.s^{-1}]

GREEK LETTERS

α	volume fraction ,[-]
β	interphase drag coefficient,[kg.m^{-3}.s^{-1}]
ε	turbulence dissipation rate ,[m.s^{-3}]
Θ_s	granular temperature,[m^2.s^{-2}]
ρ	density, [kg.m^{-3}]
λ	bulk viscosity,[Pa.s]
μ	dinamic viscosity,[kg.m^{-1}.s^{-1}]
$\overline{\overline{\tau}}$	stress tensor ,[Pa]

SUBSCRIPTS

f	final
g	gas phase
p	phase type (solid or gas)
q	phase type (solid or gas)
s	particle phase
tr	turbulent
xs	cross-sectional/projected

INTRODUCTION

Particle curtains play an important role in the drying process that occurs within flighted rotary dryers. Numerous empirical models have been developed to predict curtain solid transport (predominantly drag) (Schiller and Naumann,1933 ;Wen and Yu,1966 ;Baker,1992) and drying (i.e heat and mass transfer) (Ranz,1952). In particular, the use of single particle models is dominant.

Ogata et al. (2001) compared the behaviour of free falling curtains and single particles in a particle jet in terms of vertical velocity. It was found that the velocity of particles within curtains was higher than the velocity of comparable single particles. Ogata et al. and Hurby et al.(1988) suggested that this was due to the surrounding air being entrained within the curtain, reducing drag.

Hurby et al. (1988) studied heat transfer in freely falling curtains (0.02, 0.04 kg/s) of spherical Norton Master Beads^{TM} and compared experimental observations to 2-D Eulerian-Lagrangian simulations. The results showed that heat losses were lower at high flow rate (0.04 kg/s) when compared to low mass flow rate (0.02kg/s).

Wardjiman et al. (2008 and 2009) studied the shape of particle curtains in terms of divergence and convergence downstream of the discharge. It has been observed that varying initial curtain widths at the discharge point can lead to both diverging and converging curtain behaviour. It was found that for small initial curtain widths (i.e 2cm) the shape of the falling curtain diverged whereas at larger curtain widths (i.e 8cm) the curtain converged. The convexity behaviour has been attributed to variation in air pressure (Moore, 2010). 3D Eulerian-Eulerian CFD reported in these papers was found to reasonably match experimental results for curtain shape under both stagnant and cross flow air conditions.

Wardjiman et al. (2009) studied heat transfer in a particle curtain experimentally and numerically. Numerical study was based on the single particle model. Experiments were conducted in a rectangular tunnel in which particles were heated with hot air. Temperatures of both particles within curtain, and the gas were collected. Single particle thermal model was not well matched with air temperature from the experiments.

In this paper the Eulerian-Eulerian approach has been used to compare CFD derived heat loss in curtains, to heat loss derived using the single particle model. Conditions leading to maximum heat transfer in particle curtains are examined.

CFD MODEL

A 3-D Eulerian–Eulerian model was used to simulate gas-particle interactions in falling particle curtains. The simulations were performed using ANSYS CFX V13.0 CFD software.

The model equations in Eulerian-Eulerian approach are based on the continuity, momentum, energy conservation principles at steady state:

Continuity Equations

Gas phase:

$$\frac{\partial(\alpha_g\rho_g)}{\partial t}+\nabla.\left(\alpha_g\rho_g\vec{v}_g\right)=0, \quad (1)$$

Solid phase:

$$\frac{\partial(\alpha_s\rho_s)}{\partial t}+\nabla.\left(\alpha_s\rho_s\vec{v}_s\right)=0. \quad (2)$$

Momentum Equations

Gas phase

$$\frac{\partial}{\partial t}(\alpha_g\rho_g\vec{v}_g)+\nabla.\left(\alpha_g\rho_g\vec{v}_g\vec{v}_g\right)=\nabla.\bar{\bar{\tau}}_g-\alpha_g\nabla P-\alpha_g\rho_g\vec{g}+\beta(\vec{v}_s-\vec{v}_g), \quad (3)$$

Solid phase

$$\frac{\partial}{\partial t}(\alpha_s\rho_s\vec{v}_s)+\nabla.\left(\alpha_s\rho_s\vec{v}_s\vec{v}_s\right)=\nabla.\bar{\bar{\tau}}_s-\alpha_s\nabla P-\alpha_s\rho_s\vec{g}+\beta(\vec{v}_g-\vec{v}_s). \quad (4)$$

Stress tensors:

$$\bar{\bar{\tau}}_g=\alpha_g\mu_g(\nabla\vec{v}_g+\nabla\vec{v}_g^T)+\alpha_g\left(\lambda_g+\frac{2}{3}\mu_g\right)\nabla.\vec{v}_g\bar{\bar{I}}, \quad (5)$$

$$\bar{\bar{\tau}}_s=\alpha_s\mu_s(\nabla\vec{v}_s+\nabla\vec{v}_s^T)+\alpha_s\left(\lambda_s+\frac{2}{3}\mu_s\right)\nabla.\vec{v}_s\bar{\bar{I}}, \quad (6)$$

Bulk viscosity:

$$\lambda_s=\frac{4}{3}\alpha_s^2\rho_s d_s g_0(1+e_s)\sqrt{\frac{\Theta_s}{\pi}} \quad (7)$$

Solid pressure:

$$P_S=\alpha_s\rho_s\Theta_s(1+2g_0\alpha_s(1+e_s)) \quad (8)$$

Shear viscosity:

$$\mu_s=\frac{4}{5}\alpha_s\rho_s d_s g_0(1+e_s)\sqrt{\left(\frac{\Theta_s}{\pi}\right)}+\frac{5\sqrt{\pi}}{48}\frac{\rho_s d_s}{(1+e_s)\alpha_s g_0}[1+\frac{4}{5}(1+e_s)g_0\alpha_s]^2\sqrt{\Theta_s} \quad (9)$$

Radial distribution function Gidaspow (1994):

$$g_0=\left[\frac{3}{5}[1-\left(\frac{\alpha_s}{\alpha_{s,max}}\right)^{\frac{1}{3}}\right]^{-1}, \quad (10)$$

$\alpha_{s,max}=0.65$

Granular temperature:

$$\Theta_s=\frac{1}{3}\overline{\acute{v}_s\acute{v}_s} \quad (11)$$

Energy Equation

$$\frac{\partial}{\partial t}(\alpha_q \rho_q h_q) + \nabla.(\alpha_q \rho_q \vec{v}_q h_q) = \alpha_q \frac{\partial p_q}{\partial t} - \nabla.\vec{q}_q + Q_{pq} \quad (12)$$

In which h_q is specific enthalpy of q^{th} phase , $\nabla.\vec{q}_q$ is the heat flux and Q_{pq} is the intensity of heat exchange between the p^{th} and q^{th} phases.

Heat transfer Equations

Equations of convective heat transfer between particle curtains and air can be written as follows:

$$Q_{sg} = hA(T_s - T_g) \quad (13)$$

Where h is convective heat transfer coefficient, A is the area of particles in curtain.

$$h = \frac{Nu.k_g}{d_s} \quad (14)$$

The Ranz-Marshall correlation (Hurby et al. ,1988) was used to describe heat transfer coefficient characterising correlation between air and particles:

$$Nu = 2 + 0.6Re^{0.5}Pr^{0.3} \quad (15)$$

$$Pr = \frac{C_{pg}\mu_g}{k_g} \quad (16)$$

$$Re = \frac{\alpha_s \rho_g d_s |\vec{v}_g - \vec{v}_s|}{\mu_g} \quad (17)$$

Drag model

Interphase drag (β) is an important characteristic and has been the subject of numerous investigations (Pei et al. ,2012).The classic approach to modelling these dilute two-phase systems is the Gidaspow model which is a combination of two older model developed by Wen-Yu and Ergun(Gidaspow ,1994).

$$\beta = (1 - \varphi_{gs})\beta_{Ergun} + \varphi_{gs}\beta_{Wen-Yu} \quad (18)$$

$$\varphi_{gs} = \frac{\arctan[150 \times 1.75(0.2 - \alpha_s)]}{\pi} + 0.5 \quad (19)$$

$$\beta_{Ergun} = 150\frac{\alpha_s^2 \mu_g}{\alpha_g d_s^2} + 1.75\frac{\alpha_s \rho_g |\vec{v}_g - \vec{v}_s|}{d_s} \quad \alpha_g < 0.8 \quad (20)$$

$$\beta_{Wen-Yu} = \frac{3}{4} C_D \frac{\alpha_s \rho_g}{d_s} |\vec{v}_g - \vec{v}_s| \alpha_g^{-2.65} \quad \alpha_g \geq 0.8 \quad (21)$$

The particle drag model (C_D) was evaluated using the commonly used Schiller-Naumann equation (Schiller and Naumann ,1933):

$$C_D \begin{cases} \frac{24}{\alpha_g Re}\left[1 + 0.15(\alpha_g Re)^{0.687}\right] & Re < 1000 \\ 0.44 & Re \geq 1000 \end{cases} \quad (22)$$

Where:

$$Re = \frac{\rho_g d_s |\vec{v}_g - \vec{v}_s|}{\mu_g} \quad (23)$$

Turbulence model

The k-ε turbulence model has been frequently used for multi-phase simulation and has been shown to provide close agreement between experiments and simulations (Papadikis et al., 2009; Wardjiman et al., 2008 &2009).

Continuous phase Turbulence model ($\kappa - \varepsilon$ model)

$$\mu_{tr} = 0.09\frac{\rho k^2}{\varepsilon} \quad (24)$$

Turbulent kinetic energy

$$\frac{\partial}{\partial t}(\alpha_g \rho_g k_g) + \nabla.\left(\alpha_g(\rho_g \vec{v}_g k_g - (\mu + \frac{\mu_{tg}}{\sigma_k})\nabla k_g)\right) = \alpha_g(G_{k,g} - \rho_g \varepsilon_g) + T_{gs}^{(k)} \quad (25)$$

Turbulent dissipation rate

$$\frac{\partial}{\partial t}(\alpha_g \rho_g \varepsilon_g) + \nabla.\left(\alpha_g \rho_g \vec{v}_g \varepsilon_g - (\mu + \frac{\mu_{tg}}{\sigma_k})\nabla \varepsilon_g)\right) = \alpha_g \frac{\varepsilon_g}{k_g}(C_{\varepsilon 1} G_{k,g} - C_{\varepsilon 2}\rho_g \varepsilon_g) + T_{gs}^{(\varepsilon)} \quad (26)$$

Where $C_{\varepsilon 1} = 1.44, C_{\varepsilon 2} = 1.92, \sigma_k = 1.0\ and\ \sigma_\varepsilon = 1.3$ are constants. $T_{gs}^{(k)}$ and $T_{gs}^{(\varepsilon)}$ represent the influence of dispersed phase on the continuous phase.

Generation of turbulent kinetic energy

$$G_{k,g} = \mu_{tr,g}\nabla\vec{v}_g.\left(\nabla\vec{v}_g + \nabla\vec{v}_g^{T}\right) - \frac{2}{3}\nabla.\vec{v}_g + \left(3\mu_{tr,g}\nabla.\vec{v}_g + \rho_g k_g\right) + G_{kb,g} \quad (27)$$

Buoyancy turbulence

$$G_{kb,g} = -\frac{\mu_{tr,g}}{\rho_g} g.\nabla\rho_g \quad (28)$$

Dispersed phase Turbulence model (Zero-Equation model)

$$\mu_{tr,s} = \frac{\rho_s}{\rho_g}\mu_{tr,g} \quad (29)$$

SINGLE PARTICLE MODEL

Drag and gravitational forces are the most important forces acting on a single particle. The general equation of motion for a single particle can then be writhen as:

$$F_{net} = F_G - F_D \quad (30)$$

$$m_s\frac{dv_s}{dt} = F_G - F_D \quad (31)$$

In which:

$$F_G = m_s g \quad (32)$$

$$F_D = C_D A_{xs} \frac{1}{2} \rho_g v_s^2 \quad (33)$$

Thus:

$$m_s \frac{dv_s}{dt} = m_s g - C_D A_{xs} \frac{1}{2} \rho_g v_s^2 \quad (34)$$

The initial velocity of the single particle was assigned the same initial velocity as the curtaining particles at the inlet. Heat transfer in single particle can be described by equations (6) to (10).Therefore the temperature of a single particle was calculated by numerical integration of equation 35:

$$\frac{dT_s}{dt} = \frac{A_s \times h}{m_s \times c_p} (T_g - T_s) \quad (35)$$

In the single particle model it was assumed that the gas temperature remains constant at 300K.The drag coefficient (C_D) used in single particle model was calculated using the same relations as the Eulerian-Eulerian simulation (Equation 22).

COMPUTATIONAL SET-UP

The geometry consists of a rectangular box with varying slot width in X direction from 10 to 80 mm and constant slot length in the Z direction of 150mm (Figure 1).

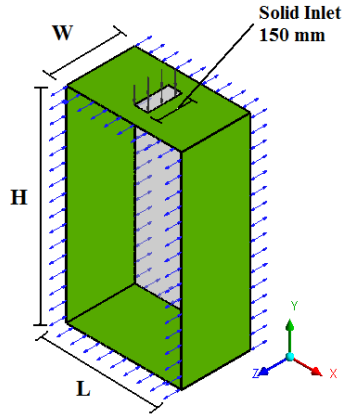

Figure 1: Schematic diagram of simulation domain (L=450 mm, H=900 mm and W=225 mm)

The model was solved with 4mm multizone mesh size. The details of mesh dependency will be described further in this paper. The simulation initial conditions are given in Table 1.

Table 1: Initial conditions of simulation domain

Solid volume fraction at solid inlet	0.52
Solid inlet temperature	400 K
Initial gas temperature	300 K
Air velocity at solid inlet	0 m/s
Solid mass flow rate at solid inlet	0.041,0.1,0.2kg/s

AVERAGE HEAT LOSS IN PARTICLE CURTAIN

The heat loss is characterised as the total heat loss of the falling particles from the entrance to the landing zone (in this case located 0.9m down from the entrance).

Equation 36 was used to determine the total heat loss per unit mass within the curtain.

$$\hat{Q} = C_p \overline{\Delta T} \quad (36)$$

Where $\hat{Q}$ is the total heat loss per unit mass, C_p is the heat capacity of sand (Incropera and DiWitt ,2002) and $\overline{\Delta T}$ is the average temperature difference within the falling height ($\bar{T}_2 - T_{inlet}$). In which $\bar{T}_2$ is the average temperature of the particle curtain in a ZX plane 0.9 m down from the entrance (Figure 2). The inlet temperature (T_{inlet}) is well-defined. The outlet temperature is more challenging to determine.

Typically integration is used for the calculation of average properties. The temperature of the particle curtain at the defined plane is described by numerical integration of the data (Equation 37), using mass flow rate as a weight function:

$$\bar{T}_2 = \frac{\int_{x=0}^{x=W} \int_{z=0}^{z=L} m^0 T_{xz} dz dx}{\int_{x=0}^{x=W} \int_{z=0}^{z=L} m^0 dz dx} \quad (37)$$

Integration can be defined as an infinite sum. Therefore the integration form can be replaced by summation of values (Equation 38).

$$\bar{T}_2 = \frac{\sum_{z=0}^{z=L} \sum_{x=0}^{x=W} m_{xz}^0 T_{xz}}{\sum_{z=0}^{z=L} \sum_{x=0}^{x=W} m_{xz}^0} \quad (38)$$

In Equations 35 and 36 m_{xz}^0 and T_{xz} are mass flow rate and temperature of sand at each node of simulation in the defined ZX plane.

In each node of the ZX plane particularly the outside edges, negative and positive values of mass flow rate occur (Figure 3). Only mass flow values for the downward particles were considered.

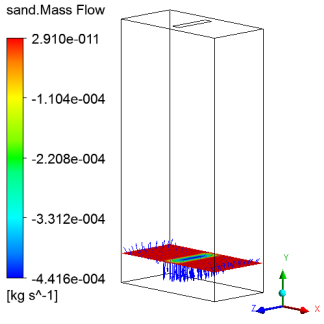

Figure 3: sand mass flow rate vectors at ZX plane, 0.9m down from the entrance

MESH DEPENDENCY

The accuracy of results depends on the quality of mesh size used in simulations. Kim et al. (2009) investigated mesh dependency in their modelling of a pilot scale solid particle receiver. It was found that mesh size in the CFD simulation

has an important effect on determining the thickness of the curtain.

In this paper mesh dependency was carried out on the described geometry at different mesh sizes (3mm,4mm,5mm,6mm,7mm and 8mm) with a mass flow rate of 0.041kg/s .Different slot sizes (10mm, 60mm and80 mm) were investigated (Figure 4).Average heat loss per unit mass as, described in equation 34,was used as the convergence criteria. A mesh size of 4 mm with 1,449,225 elements was utilised in all simulations.

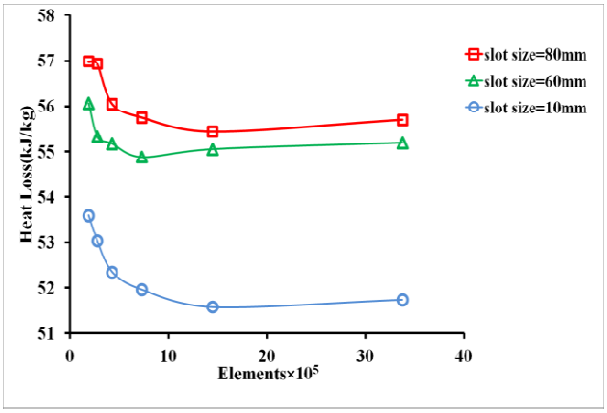

Figure 4: Heat loss predictions using the indicated element sizes

RESULTS

Figure 5 shows a selection of results comparing CFD calculated heat losses per unit mass at different slot sizes (10mm, 30mm, 60mm and 80 mm), mass flow rates (0.041kg/s, 0.1kg/s and 0.2 kg/s) and particle sizes (0.2mm, 0.4mm and 0.6mm). Similar trends in the effect of particle size (0.041 kg/s) were observed at higher mass flow rates of 0.1kg/s and 0.2 kg/s.

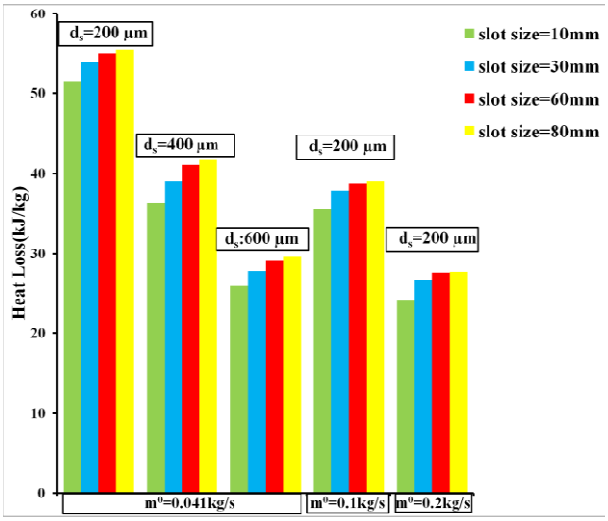

Figure 5: Heat loss comparison at slot sizes of 10mm, 30mm, 60mm, 80mm, particle sizes of 0.2mm, 0.4mm and 0.6mm and mass flow rates of 0.041kg/s,0.1kg/s and 0.2kg/s

Wardjiman et al. (2009) used sampling cups to obtain temperatures versus curtain height at a single location. As such the bulk temperature profile across the entire curtain was not obtained. Although the modelling work in this paper is qualitatively well matched to the effect of mass flow rate on particle temperature profiles (Hurby et al. (1988)), it is important to obtain bulk temperatures maps of the entire curtain. In a follow-up paper by the authors the experimental technique will be used for validation of these simulation results. This is the subject for the future study.

Figure 6 shows a comparison of heat loss per unit mass versus slot widths at the different mass flow rates for particle size of 200 µm. It was observed that there is a critical condition upon which further increases in slot width do not lead to increases in heat loss per unit mass. It can be seen that heat loss is higher at lower mass flow rate (0.041kg/s), however heat loss is almost independent of slot size at larger slot sizes of 60mm and 80mm in the same mass flow rate.

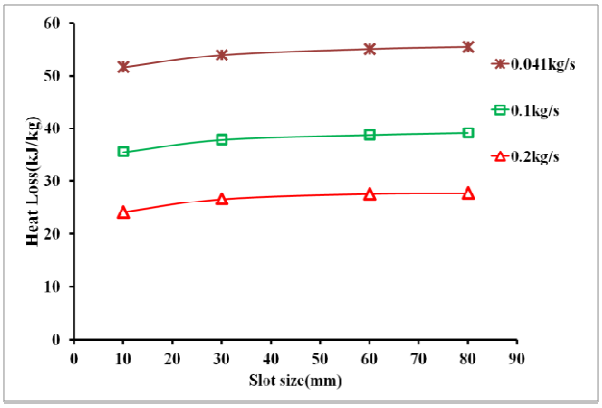

Figure 6: Heat loss per unit mass for different slot sizes at mass flow rates of 0.041kg/s .0.1kg/s and 0.2kg/s for partilce size of 200µm

Figures 7-9 shows the temperature comparison between single particle simulations and CFD values for the centreline temperature of particles in the curtains. The temperature of single particle and particles in curtain has been non-dimensionalized :$T^* = \frac{T-T_{f-CFD}}{T_0-T_{f-CFD}}$,in which $T_{f\text{-}CFD}$ is the final temperature of particles in curtain after 0.9 m falling distance and T_0 is 400 K.

It was found that the heat loss per unit mass of particles in curtain is less than the single particle particularly at higher mass flow rates (0.1kg/s and 0.2kg/s) and there are smaller temperature differences between single particle simulations and CFD results for particles in the curtain at low mass flow rate (0.041kg/s).

It can be seen that for narrow slots (10mm), in all cases the single particle loses heat faster than its equivalent curtain. As the slot width widens or mass flow rate decreases this effect is less pronounced. In fact, in the low mass flow rate (0.041kg/s) and wide slot (60 and 80 mm)simulations this effect is reserved and the single particle loses heat at a slower rate. Under these low flow, wide slot conditions the curtain shape is convergent (narrows as it falls) rather than divergent, which seems to be a significant factor.

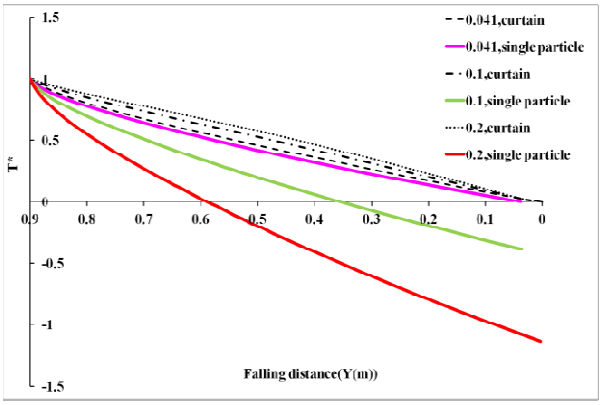

Figure 7: Temperature comparison between single particle and particles in curtain in 10 mm slot at three 0.041, 0.1 and 0.2 kg/s mass flow rates and particle size of 200µm

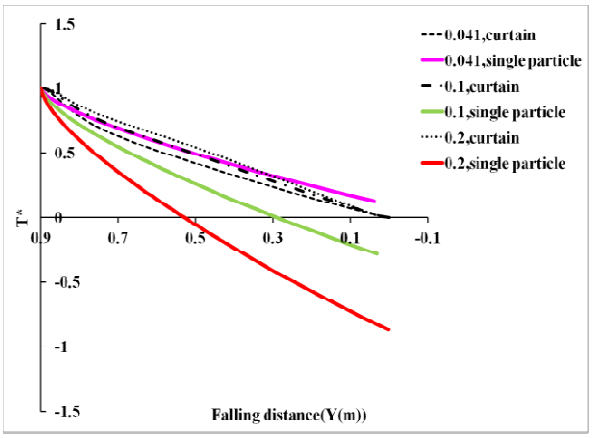

Figure 8: Temperature comparison between single particle and particles in curtain in 60 mm slot at three 0.041, 0.1 and 0.2 kg/s mass flow rates and particle size of 200µm

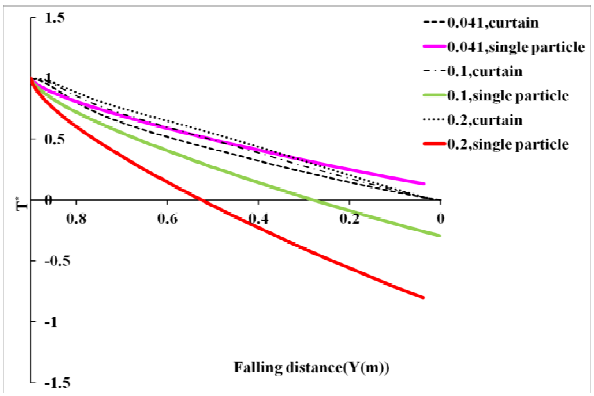

Figure 9: Temperature comparison between single particle and particles in curtain in 80 mm slot at three 0.041, 0.1 and 0.2 kg/s mass flow rates and particle size of 200 µm

CONCLUSION

CFD simulations have been used to predict the heat transfer and temperature profiles within particle curtains with different mass flowrates (0.041kg/s,0.1kg/s,0.2kg/s) discharging through different widths slots (10mm,60mm,80mm). The CFD results have been compared to the temperature of single particle falling under equivalent conditions. It was found that the heat loss within the particle curtains is less than the equivalent single particle heat loss, as expected. As the mass flow rate of the particle curtains increases, the rate of heat loss decreases. Heat loss per unit mass decreased by a maximum of 13% by decreasing curtain width from 80mm to 10mm.However, CFD simulations show that there is a limit to the potential increase in heat transfer as initial curtain width increases.

REFERENCES

BAKER, C.G.J. ,(1992), “Air-solids drag in cascading rotary dryers”, *Drying Technol.: An International Journal*, **10**,365 - 393.

GIDASPOW, D. ,(1994), *Multiphase Flow and Fluidization.Academic Press*. San Diego.

HURBY, J., STEEPER,R., EVANS,G., AND CROWE,C. ,(1988), “An experimental and numerical study of flow and convective heat transfer in freely falling curtain of particles”, *J. Fluid Eng.*,**110**,172-181.

INCROPERA, F.P.AND DEWITT,D.P.,(2002), *Fundamentals of Heat and Mass Transfer*: John Wiley & Sons,Inc.

KIM, K., SIEGEL, N., KOLB ,G., RANGASWAMY ,V., AND MOUJAES ,S.F., (2009), “A study of solid particle flow characterization in solar particle receiver” *Sol. Energy*, **83**(10),1784-1793.

MOORE, A. ,(2010), “Heat transfer analysis of a particle curtain using Computational Fluid Dynamic”, Chemical Engineering, James Cook University.

PAPADIKIS, K., GU, S., AND BRIDGWATER, A.V. ,(2009), “CFD modelling of the fast pyrolysis of biomass in fluidised bed reactors. Part B: Heat, momentum and mass transport in bubbling fluidised beds”, *Chem. Eng. Sci.*, **64**(5),1036-1045.

PEI, P., ZHANG, K., AND WEN, D. ,(2012), “Comparative analysis of CFD models for jetting fluidized beds: The effect of inter-phase drag force”,*Powder Technol.*, **22**,114-122.

RANZ, W.E. ,(1952), “Friction and transfer coefficients for single particles and packed beds”, *Chem. Eng. Prog.*, **48**,247-253.

SCHILLER, L.AND NAUMANN ,A., (1933), “Über die grundlegenden Berechnun gen bei der Schwekraftaubereitung ”, *Z. Ver.Dtsch. Ing.*,**77**,318-320.

WARDJIMAN, C., LEE ,A., SHEEHAN ,M., AND RHODES, M.,
(2008), “Behaviour of a curtain of particles falling through a horizontally-flowing gas stream”, *Powder Technol.*, **188**,110-118.

WARDJIMAN, C., LEE ,A., SHEEHAN ,M., AND RHODES, M. (2009), “Shape of a particle curtain falling in stagnant air”, *Powder Technol.* ,**192**,384-388.

WARDJIMAN,C. AND RHODES, M. ,(2009),“Heat trasnfer in a particle curtian falling through a horizontally-flowing gas stream”,Powder Technol.,**191**,247-253.

WEN, C.Y.AND Y.H. YU. ,(1966) “Mechanics of fluidization”, *AIChe Symposium Series*, **62**,100-111.

ZHANG, K., ZHANG, J., AND ZHANG ,B.,(2004), “CFD simulation of jet behaviour and voidage profile in a gas–solid fluidized bed”, *Int. J. Energy Res.*, **28**,1065–1074.